Electrolysis of natural waters contaminated with transition metal ions: identification of a metastable FePb-based oxygen evolution catalyst operating in weakly acidic solutions

Shannon A. Bonke,[a,b] Ken L. Abel,[c] Dijon A. Hoogeveen,[a] Manjunath Chatti,[a] Thomas Gengenbach,[d] Maxime Fournier,[a] Leone Spiccia,[a] and Alexandr N. Simonov*[a]

Vale, Leone. Thank you for all the inspiration and wisdom you shared with us.

Abstract: The possibility of efficient water electrooxidation sustained by continuous (re)generation of catalysts derived from the oxidative electrodeposition of transition metal contaminants is examined herein for three natural water samples from Australia and China. The metal composition of the solutions has been determined by ICP-OES, and a range of strategies to produce water-splitting catalysts *via in situ* electrodeposition have been applied. The performance of the resulting electrocatalysts is below the state-of-the-art level due to high amounts of impurities in the solutions and non-optimal concentrations of naturally available catalyst precursors. Nevertheless, these studies have identified the FePb-based system as a rare example of an electrocatalyst for water oxidation that forms *in situ* and maintains reasonable activity (≥4.5 mA $cm^{-2}_{geom.}$ at an overpotential of 0.8 V) in weakly acidic solutions (pH 2.9).

Introduction

The requirement for active catalysts to enable the energy efficient production of *solar fuels*, specifically, *via* the electrolytic splitting of water into O_2 and H_2 (Equation 1), has prompted extensive studies on the oxygen and hydrogen evolution reactions (OER, Equation 2 and HER, Equation 3).[1]

$$2\ 2H_2O \rightleftharpoons O_2 + 2H_2 \quad \text{(Eq. 1)}$$

$$2\ 2H_2O \rightleftharpoons O_2 + 4H^+ + 4e^- \quad \text{(Eq. 2)}$$

$$4H^+ + 4e^- \rightleftharpoons 2H_2 \quad \text{(Eq. 3)}$$

Identifying first row transition metal compounds that effectively catalyse the half-reactions in Equations 2 and 3,[2] fulfils a key requirement for materials that will ideally be used on a global scale, *viz.* composed of Earth-abundant elements. Among other strategies, fabrication of such catalysts *via* electrodeposition has generated extensive interest.[3] This method enables formation of the catalytic materials *in situ* under turnover conditions, thereby ensuring their thermodynamic stability. This approach has been extensively scrutinised in the past decade for the anode half-reaction, with crucial reports made by Nocera and colleagues on non-stoichiometric oxides of Co,[4] Ni,[5] and Mn,[6] as 'self-healing' OER catalysts. On the cathode side, *in situ* electrodeposited transition metal catalysts have attracted less attention in the light of the exceptional activity and stability of Pt, as well as the promising performance of catalytic materials based on metal chalcogenides and phosphides.[7]

Importantly, active water oxidation electrocatalysts can be produced even with very low concentrations of transition metal cations in electrolysed solutions. For example, the formation of CoO_x has been shown from Co^{II} salt impurities in solutions of cobalt complexes that were initially designed to function as molecular OER catalysts.[8] Incorporation of iron into the structure of NiO_x from hard to detect impurities in electrolyte solutions, to form the much more active $FeNiO_x$ OER catalyst has recently been unambiguously proven.[9] Furthermore, electrodeposition of an active nickel-based OER catalyst has been reported from 'blank' solutions containing only 17 nM of adventitious Ni^{2+}.[10] Similar unsuccessful control 'blank' measurements, where undesired admixtures compromised the result, have likely occurred in other laboratories yet simply remain unpublished.

Low concentrations of transition metal ions are typical in wastewater that is legally diluted into natural water sources in many countries. Electrochemical conversion of these cations into OER and/or HER catalysts would allow for the *in situ* creation of anodes and cathodes for water splitting without the need to pre-synthesise the materials, while also functioning to purify the waste water. This approach could provide obvious environmental benefits as it would allow the collection of pollutants and conversion thereof into useful materials. The plausibility of this strategy is assessed herein.

Results and Discussion

Water taken from natural sources contains a vast number of organic and inorganic species, and the selection of samples from rivers that contain runoff from mining operations rendered them likely to contain transition metal cations. Herein, samples were obtained from rivers in the Luina and Queenstown regions of Tasmania, Australia and from East Lake in Wuhan, China. The latter has been recently reported as being polluted.[11]

[a] Dr. S. A. Bonke, Dr. D. A. Hoogeveen, M. Chatti, Dr. M. Frounier, Prof. Dr. L. Spiccia, Dr. A. N. Simonov
School of Chemistry and the ARC Centre of Excellence for Electromaterials Science,
Monash University
Victoria 3800, Australia
E-mail: alexandr.simonov@monash.edu
[b] Dr. S. A. Bonke
Institut Nanospektroskopie,
Helmholtz-Zentrum Berlin für Materialien und Energie,
Kekuléstraße 5, 12489 Berlin, Germany
[c] K. L. Abel
Fakultät für Chemie und Mineralogie
Universität Leipzig,
Johannisallee 29, 04103 Leipzig, Germany
[d] Dr. Thomas Gengenbach
Commonwealth Scientific and Industrial Research Organisation
Victoria 3168, Australia

Supporting information for this article is given via a link at the end of the document.

Inductively coupled plasma optical emission spectrometric (ICP-OES) analysis of the examined samples indicates that water from rivers in the mining areas in Australia contains suitable ions for electrodeposition of catalysts for water splitting (Table 1). Specifically, Ni and Co are present at the μM level with significantly higher concentrations (*ca* 10^3 μM) of Fe and Mn observed. Although the relative amounts might not be ideal, the key components are available and therefore electrodeposition of OER and HER catalysts might be possible. Significantly lower concentrations of the probed metals were detected in the Wuhan lake sample.

Table 1. Concentration (μM) of selected elements in natural water samples as determined by ICP-OES.[a]

Element	Wuhan	Queenstown	Luina
Ca	920	2700	1400
Mg	380	8200	1700
Zn	<0.1	80	620
Al	16	3300	910
Pb	<0.1	0.5	2.2
Cr	<0.1	0.6	0.4
Fe	3.8	2900	49
Mn	0.4	1300	78
Co	<0.2	20	0.9
Ni	<0.1	3.6	6.7

[a] Ti, Mo and Sn were below their detection limits in all samples (<0.1, <0.4, and <0.3 μM, respectively).

Electrolysis of natural waters. *In situ* generation of water electrooxidation catalysts was attempted in the examined water samples with added supporting electrolyte by applying positive potentials, following a well-established strategy of generating 'self-healing' electrocatalysts.[4c, 12] This was undertaken in both potentiodynamic (voltammetric) and potentiostatic (chronoamperometric) modes, since for example, deposition of "active" MnO_x catalysts requires cycling the potential,[13] while efficient CoO_x and NiO_x can be formed in both regimes.[4-5] For the supporting electrolyte, either sodium sulphate (0.2 M, pH adjusted within the 2.3 to 2.9 range) or borate buffer (0.1 M, pH 9.2) were employed. The Luina and Queenstown samples contained naturally occurring precipitates and were weakly acidic (pH of *ca* 3), with alkalisation expectedly resulting in further sedimentation of poorly soluble hydroxides of the metals present (Table 1). These solids were filtered out using a 20 μm syringe filter and electrochemical experiments were undertaken with the resulting transparent solutions.

In a typical voltammetric experiment for transition-metal-catalysed water oxidation with or without concomitant electrocatalyst deposition, applying an increasingly positive potential first induces redox transformations of a catalyst and/or dissolved precursor followed by oxidation of the solvent. This is exemplified in Figure 1A for borate-buffered Luina and Queenstown samples examined using F-doped SnO_2 electrodes (F:SnO_2). The solubility of transition metal cations is sufficient to electrodeposit OER catalysts in borate buffered media (pH 9.2).[4b, 5, 13] Consistent with the ICP-OES results, the processes preceding the water oxidation wave resemble those observed for MnO_x,[14] and increase with subsequent cycles under stirred conditions indicating the deposition of electroactive species on the electrode (Figure S1). This was corroborated by the formation of pale yellow coatings during chronoamperometric depositions (Figure 1B). These deposits were comprised of Mn-containing aggregates as revealed by scanning electron microscopy and local energy dispersive X-ray (EDX) analysis (Figure 2). Aside from the signals from a clean F:SnO_2 surface, only Mn could be detected in the produced films by EDX.

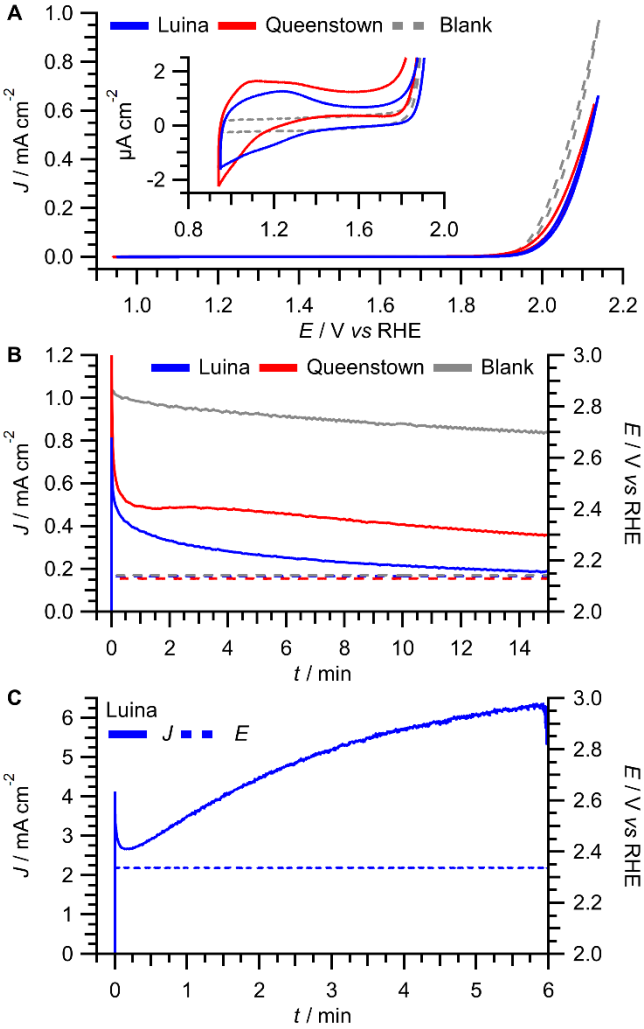

Figure 1. (**A**) Cyclic voltammetric (scan rate 0.020 V s^{-1}) oxidation of borate buffered (0.1 M, pH 9.2) Luina (*blue*) and Queenstown (*red*) river samples alongside deionised (DI, 18.2 MΩ cm) water (*dashed grey*), with inset enhanced plot of the processes preceding the water oxidation wave; and (**B**) chronoamperometric (E = 2.14 V) oxidation of those solutions. (**C**) Chronoamperometric (E = 2.34 V) oxidation of an acidified Luina sample with added Na_2SO_4 (0.2 M, pH 2.9). Experiments were undertaken using F:SnO_2 electrodes in quiescent, air saturated solutions. *Solid* and *dashed* lines in panels **B** and **C** show current and potential response, respectively.

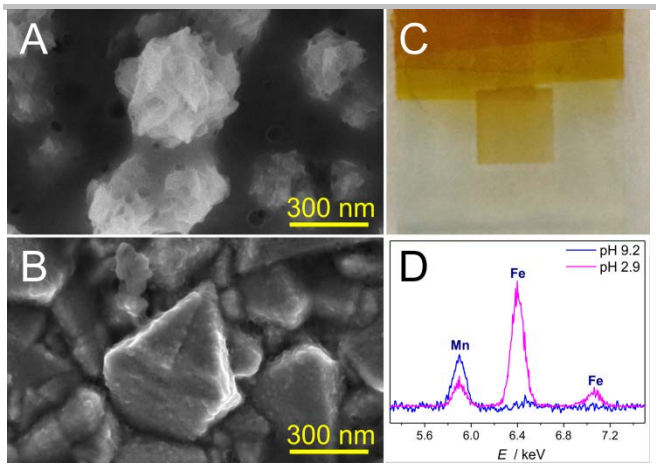

Figure 2. (**A**, **B**) Scanning electron micrographs of the deposits produced on a F:SnO_2 electrode by chronoamperometric oxidation of Luina water with added (**A**) 0.1 M borate buffer, pH 9.2; or (**B**) 0.2 M Na_2SO_4, pH 2.9 (in the latter case, the electrodeposited material is a coating covering the F:SnO_2 crystals). Photograph of the deposit obtained at pH 9.2 is shown in panel (**C**). Panel (**D**) shows fragments of the EDX spectra within the energy range corresponding to Mn and Fe.

However, the formation of this material does not facilitate the electrooxidation of water, but on the contrary, it suppresses the catalytic activity of the F:SnO_2 electrode. This trend is mirrored in chronoamperometric deposition at very positive potentials sufficient to oxidise water, *viz.* 2.13-2.14 V *vs*. the reversible hydrogen electrode (RHE), where a gentle decay in the oxidative current over time is observed (Figure 1B). This is also supported by voltammetric analysis of the deposited films in borate buffer solutions prepared with reverse osmosis purified (RO, 1 MΩ cm) water (Figure S1).

The use of the Wuhan water sample resulted in a minor improvement of the water oxidation activity of F:SnO_2 under voltammetric conditions, though applying constant positive potentials did not enhance the performance further (Figure S2). Additionally, these measurements did not induce the formation of detectable metal oxide deposits, which is in contrast to the Luina and Queenstown waters. This is probably a consequence of the significantly lower concentrations of the transition metal contaminants in the water (Table 1), with the lower Mn content clearly visible in the voltametric response.

Blank/Control experiments undertaken with deionised (DI, 18.2 MΩ cm) water did not show extraneous processes and only allowed water oxidation at very positive potentials, which slowly decayed over time, presumably due to degradation of the F:SnO_2 support under the harsh oxidative conditions employed (Figure S3). Similar behaviour was also found in many control experiments undertaken with reverse osmosis purified water (Figure S4), which contained no admixtures at concentrations exceeding the ICP-OES detection limits (see Experimental). However, evolution of voltammetric response(s) prior to the water oxidation wave and an undesired enhancement in activity was observed in some measurements using “pure” RO water solutions (Figure S5), notwithstanding extensive washing of the labware and the use of high quality reagents. This observation provides an additional warning that the use of ultra-pure DI water is always desirable in electrochemical experiments and emphasises the importance of undertaking control measurements along with the actual experiments to confirm a satisfactory level of purity.

Although active Co and Ni oxide catalysts can be theoretically obtained from the alkaline solutions of the examined mining water samples, their formation is obviously hindered by the presence of undesired cations. Indeed, iron and manganese dominate the electrodeposited product (Figures 1 and 2), notwithstanding that their concentrations should significantly decrease upon alkalisation to become closer to the concentrations of cobalt and nickel. The water oxidation activity of $MnFeO_x$ derived from the borate buffered Luina and Queenstown samples tested in both natural waters, and pure electrolyte solutions is very low (Figure 1A, 1B and Figure S1). No improvements in the performance could be achieved upon application of the electrochemical activation procedures previously introduced to enhance the water oxidation activity of electrodeposited MnO_x.[15]

In principle, introducing ammonia into the solutions can significantly and selectively suppress the concentrations of dissolved Mn and Fe, while avoiding precipitation of the more catalytically relevant Co and Ni. This is because coordination of NH_3 by nickel and cobalt cations forms water soluble complexes, while manganese and iron precipitate as hydroxides due to the pH increase.[16] However, such treatment of the Luina sample and subsequent removal of the resulting precipitate by filtration (final pH 9.9 with 0.2 M Na_2SO_4) did not allow the deposition of more electrocatalytically active materials by voltammetry or chronoamperometry. This was demonstrated by cyclic voltametric analysis of quiescent and stirred NH_3-treated solution, chronoamperometric deposition from this solution, and cyclic voltammetry of the deposited film in a DI water solution (Figure S6A-D). Once again, the water oxidation current was lower with each voltammetric cycle and also decayed under potentiostatic oxidative conditions indicating passivation of the electrode surface. Cyclic voltammograms of the produced films in both pure borate buffer and NaOH solutions indicated the formation of a MnO_x-based film.

Thus, the materials electrodeposited from the water samples examined herein under weak alkaline conditions are dominated by manganese and iron. Moreover, this is unavoidable without advanced purification procedures, which would be industrially unfavourable. Oxides/oxyhydroxides of these metals have been shown to function as water oxidation catalysts,[6, 17] as were their combinations,[18] though relatively low activity was reported for $MnFeO_x$ in a recent publication.[3] However, the electrocatalytic performance for water oxidation appears to be substantially suppressed in the natural waters. One plausible reason might be the abundance of alkaline-earth metals in the solutions (Table 1), which can deposit as poorly conducting and/or catalytically inactive hydroxides on the electrode surface thereby degrading the activity.[19] In principle, this can be mitigated by undertaking water oxidation / catalyst deposition in acidic media, where Mn-based OER catalysts have also been previously reported to exhibit reasonable activity.[6] Additionally, water electrolysis at low pH is more technologically attractive than in alkaline solutions, and development of robust, self-healing OER catalysts for acidic conditions has been identified among the topical problems of solar fuel research.[20]

To this end, river water samples were acidified prior to filtering for particulates, with a redox-inactive salt lastly added as a supporting electrolyte (Na_2SO_4, 0.2 M). Under both voltammetric and chronoamperometric conditions, the OER performance of blank F:SnO_2 significantly enhanced during oxidation of the acidic Luina water sample (pH 2.9; Figure S7A-F). However, the catalytic material formed under these conditions dissolves back into the solution once the electrochemical measurements cease

(Figure S8). Continuous electrolysis of the stirred Luina solution at the very positive potential of 2.34 V *vs*. RHE (OER overpotential, η *ca* 1.11 V) provided a well-known current-time transient where oxidative current progressively grows and achieves a quasi-steady-state value, of approximately 6.0-6.3 mA cm^{-2} (Figure 1C). The resulting catalytic material was found to decorate the F:SnO_2 grains as a thin heterogeneous film that mainly contains iron and manganese (Figure 2).

This rate of the OER, provided by oxidation of the acidified Luina water sample, is significantly better than the performance reported for pure electrodeposited MnO_x during oxidation of the DI water at pH 2.5 (phosphate electrolyte), where an overpotential of up to 1.0 V was required to sustain the current density of only 0.1 mA cm^{-2}.[20a] However, the same work also reports on a significantly more active ternary $CoFePbO_x$ system, which enables 1 mA cm^{-2} water oxidation current density at η = 0.57 V at pH 2.0 (Na_2SO_4 electrolyte). Even more impressive activity for the OER was reported at more acidic pH, in particular for anodes prepared using Ti-modified MnO_2 (6 mA cm^{-2} at η = 0.67 V; 0.05 M H_2SO_4),[21] Co_3O_4 (10 mA cm^{-2} at η = 0.57 V; 0.5 M H_2SO_4),[22] and MoS_2 and TaS_2 (10 mA cm^{-2} at η = 0.5-0.6 V; 0.5 M H_2SO_4).[23] These comparisons confirm that the performance achieved herein, with the catalyst formed *in situ* and operated in natural water conditions, is surpassed by the catalytic activity of materials prepared and tested under clean conditions. Nevertheless, the material obtained from and tested in the Luina sample provides a rare example of a water oxidation catalyst that can be formed *in situ* under acidic conditions. One of the few reported similar systems employed a cobalt-based catalyst formed during oxidation of aqueous solutions containing Co^{2+} and phosphate, requiring an overpotential of 0.57 V to achieve a water oxidation current density of *ca* 0.4 mA cm^{-2} in pH 1.6 solution.[24] Interestingly, testing the weakly acidic Queenstown sample following the protocol employed for the Luina water did not produce continuous enhancements in performance (Figure S7). One plausible reason for this difference is the significantly higher concentration of manganese and alkaline earth metals in the Queenstown sample (Table 1), which appear to suppress the OER activity.

Subsequent testing of the materials oxidatively electrodeposited from slightly acidic natural Queenstown and Luina waters in 0.1 M NaOH or 0.1 M borate buffer solutions prepared with RO water confirmed their improved catalytic activity for water oxidation (Figure S9). Depositions were also carried out cathodically to reduce metals onto the electrode, which would then form oxides during the application of anodic potentials during testing. The catalytic performance achieved in this case was again higher than blank F:SnO_2, and comparable or lower than for the electrodes modified by oxidative depositions (Figure S9).

Materials reductively electrodeposited from the examined waters onto a glassy carbon electrode were also briefly tested as catalysts for H_2 evolution in clean RO water (0.2 M Na_2SO_4, pH 5.8). Slight enhancements in the electroreduction activity *vs.* an unmodified electrode were observed. However, the performance was typically very poor and also unstable even on the short time scale of voltammetric measurements (Figure S10).

Electrooxidation of "artificial" natural water. To verify the origin of the OER catalytic activity found with the acidic Luina river water, electrooxidation of DI water solutions that mimic the transition metal composition of the natural sample was examined (chronoamperometric and voltammetric data are exemplified in Figure 3 and Figure S11, respectively). In these experiments, aqueous 0.2 M Na_2SO_4 with pH 2.9 and containing mixtures of Fe^{2+} + Mn^{2+}, Fe^{2+} + Pb^{2+}, Fe^{2+} + Pb^{2+} + Ni^{2+}, or Fe^{2+} + Pb^{2+} + Ni^{2+} + Mn^{2+} were employed as electrolyte solutions. When present, the cation concentrations were 45 µM Fe^{2+}, 2 µM Pb^{2+}, 6 µM Ni^{2+} and 70 µM Mn^{2+}.

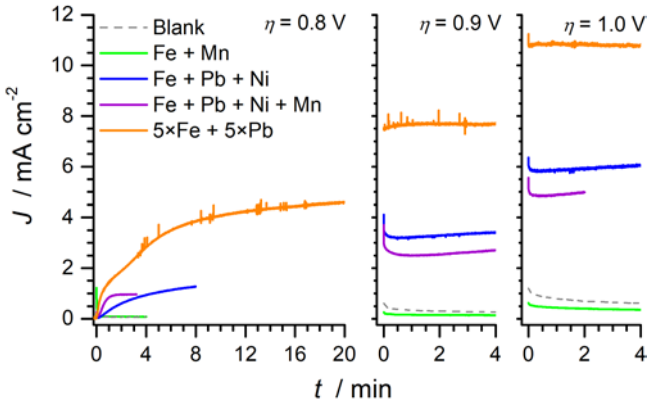

Figure 3. Chronoamperometric oxidation of DI water solutions mimicking the natural Luina water sample, containing different combinations of Fe^{2+} (45 µM), Pb^{2+} (2 µM), Ni^{2+} (6 µM) and/or Mn^{2+} (70 µM), with Na_2SO_4 (0.2 M pH 2.9) present in all cases. Additional experiment was undertaken with a 225 µM Fe + 10 µM Pb combination (labelled as 5×Fe + 5×Pb in the plot). Potential steps were applied sequentially to the same electrodes (*E* = 2.03, 2.13 and 2.23 V). Experiments were undertaken using F:SnO_2 electrodes in air saturated, stirred solutions. The electrode analysed in Fe^{2+} + Pb^{2+} + Ni^{2+} was kept with no potential applied for 5 min to allow dissolution of the catalyst and was then used for the measurements with Mn^{2+} added to the solution. Currents are normalised to the geometric surface area of the electrodes.

No activity enhancement was possible with the Mn^{2+} + Fe^{2+} combination, although facile formation of the (meta)stable $Mn(Fe)O_x$ film on the F:SnO_2 surface at potentials ≥2.03 V *vs.* RHE was detected visually and voltammetrically (Figure S11B). Conversely, the use of manganese-free mixtures Fe^{2+} + Pb^{2+} and Fe^{2+} + Pb^{2+} + Ni^{2+} produced qualitatively similar behaviour to that found with the natural Luina sample, *viz.* continuous enhancement of the oxidative current at potentials equal to and more positive than 1.93 V *vs.* RHE (data shown for the Ni-containing solution only in Figure 3 and Figure S11). The catalytically active material formed under these conditions was unstable without the application of a strongly oxidative potential, as evident by comparison of the current densities at the same potential between the chronoamperometric data and the subsequently measured cyclic voltammogram (*cf.* Figure 3 and Figure S11B). Interestingly, adding Mn^{2+} to the Fe^{2+} + Pb^{2+} + Ni^{2+} mixture enables faster stabilisation of the current density, though at lower values when η = 0.8 V. Lower current densities were observed with the Mn^{2+}-containing solution at higher overpotentials as well, indicating the presence of manganese is not beneficial to the catalytic system. The above observations suggest that electrooxidation of Mn^{2+} does not produce an active water oxidation catalyst in weakly acidic solutions, but passivates the electrode surface and prevents further formation of the catalytically active FePb(Ni)-based material.

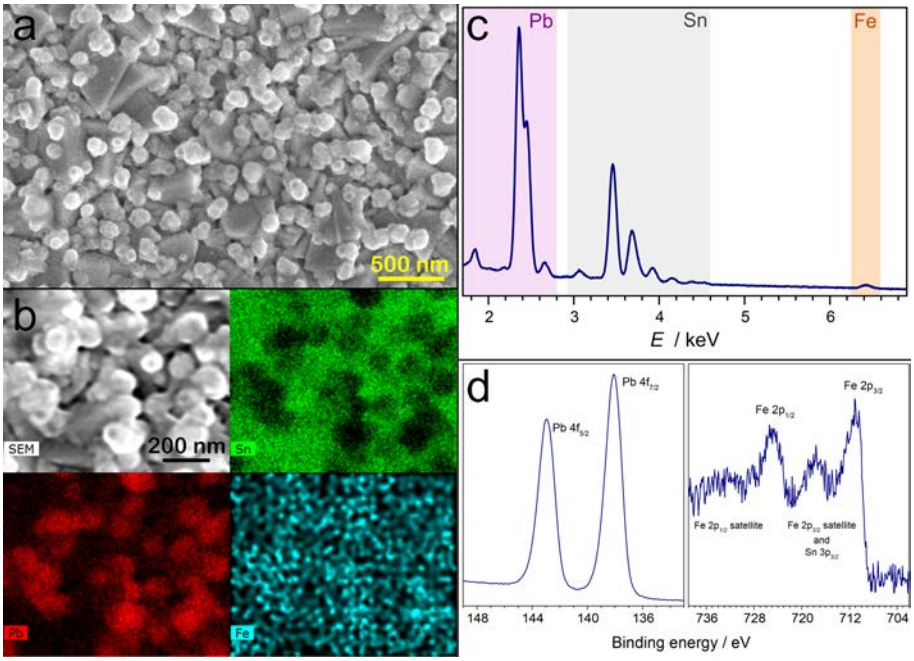

Figure 4. Characterisation of the electrodeposit produced during oxidation of aqueous 225 μM Fe^{2+} + 10 μM Pb^{2+} (with 0.2 M Na_2SO_4, pH 2.9) at 2.03 V *vs.* RHE for 20 min with a FTO electrode: (a) SEM image, (b) EDX mapping, (c) EDX spectrum, (d) Pb 4f and Fe 2p spectra.

When using Fe^{2+} and Pb^{2+} precursor concentrations similar to those found in the Luina sample (*viz.* 45 and 2 μM, respectively), the FePb(Ni) catalytic system formed *in situ* is capable of water oxidation at a rate above 1.2 mA cm^{-2} at an overpotential of 0.8 V in pH 2.9 solutions. Increasing the concentration of iron and lead salts by a factor of five enhanced the catalytic activity up to 4.7 mA cm^{-2} at η = 0.8 V (Figure 3). Quantification of the molecular oxygen evolved during these experiments confirmed close to 100% faradaic efficiency of the oxygen evolution reaction provided by the FePb-based catalyst (Figure S12). Importantly, the conditions employed herein to test the FePb(Ni) catalyst were inspired by the natural Luina water sample, and it is probable to expect that significantly better performance is possible upon future optimisation.

Characterisation of the deposits produced on the FTO surface during oxidative electrolysis of the iron- and lead-containing Na_2SO_4 solutions by X-ray photoelectron spectroscopy (XPS) and EDX revealed that the materials predominantly contain lead (hydr)oxides. Given that the size of the deposited particles is less than 1 μm (Figure 4a shows SEM image; Figure 4b shows elemental mapping data), the EDX analysis showing the Pd : Fe ratio of approximately 4 : 1 was considered to represent the bulk composition of the catalysts (Figure 4c). Detection of iron by XPS in the coating obtained with the 45 μM Fe^{2+} and 2 μM Pb^{2+} solution was hindered by strong interference from the background tin signal (Figure 4d). Increasing the thickness of the catalyst layer by using electrolyte solutions with 5-fold higher precursor concentrations (225 μM Fe^{2+} + 10 μM Pb^{2+}) produced a sample with an XPS-detectable amount of Fe and a surface lead : iron ratio of *ca* 3.4 : 1. These results are not unexpected, as lead(IV) oxide is thermodynamically stable at very positive potentials even in acidic solutions, while iron is predicted to be mainly present as soluble FeO_4^{2-} species under the conditions employed herein.[20a] The potentials required to initiate the formation of catalytically active electrodes with the Fe+Pb solutions (Figure 3) can be connected to the Pourbaix diagrams provided in Ref.[20a] Comparisons of these data suggest that water oxidation requires the formation of Fe^{4+}, while Fe_2O_3 does not sustain fast kinetics of the OER. We hypothesise that lead oxides serve as a stable solid matrix that incorporates catalytically active iron sites. Bimetallic Fe-Pb interfaces might also contribute to the catalysis, but this cannot be either confirmed or disproved by the preliminary characterisation data reported herein. Further studies, preferably using *in situ* spectroscopic analysis are required to derive deeper insights into the nature of the active sites in the $FePbO_x$-based water oxidation catalyst.

Conclusions

The results presented herein further emphasise hurdles associated with the electrolysis of water obtained from natural sources, which would be industrially favourable as it excludes the need for water purification. The presence of precursors for efficient ‘self-healing’ water oxidation catalysts based on transition metal oxides/oxyhydroxides in the electrolysed solution does not guarantee satisfactory performance, as was demonstrated herein for the Mn-, Fe-, Co- and Ni- contaminated waters. The data obtained suggest that even an initially very active catalyst, like NiFe- or Co(Fe)- based systems will eventually degrade in a contaminated natural environment, as the electroactive surface will become dominated with less active transition metal oxides. The impact of other components present, especially alkaline-earth metal cations and organic contaminants, must be considered as well. Efforts to produce efficient water oxidation catalysts *via* oxidative and reductive electrodeposition from weakly alkaline natural waters did not enable improvements in water oxidation activity. On the other hand, progressive

improvement in the reaction rate was observed at pH 2.9 in Luina river water. Under these acidic conditions, FePb(Ni)-based electrodeposits were identified as materials with a capacity to function as self-healing water oxidation catalysts. The presence of excessive amounts of manganese in solutions was found to be pernicious, notwithstanding previous reports on reasonable catalytic activity of MnO_x for water electrooxidation at low pH. Future mechanistic and optimisation studies are anticipated to significantly improve the performance of the discovered catalyst for the oxidation of acidic water.

Experimental Section

Materials. Reagent or analytical grade chemicals were used as received from commercial suppliers. Fluorine doped tin oxide coated glass with a sheet resistance of 8 Ω square^{-1} was sourced from *Dyesol Ltd.* (TEC8 Glass Plates). Reverse osmosis purified water (quoted resistivity of 1 MΩ cm at 25 °C) or ultra-pure deionised water (*Milli-Q*; quoted resistivity 18.2 MΩ cm at 25 °C) was used in the preparation of solutions excluding those composed of natural water samples. Borate buffer solutions were prepared from $Na_2B_4O_7.10H_2O$.
The Queenstown sample was collected from the Queen river at 42°4'27" S 145°33'32" E in Feb 2012. The Luina sample was obtained from the Heazlewood River at 41°26'15.2" S 145°20'46.07"E in Feb 2012. The Wuhan sample was collected from Dong Hu Chu Cheng (East lake) at 30°33'21.8" N 114°20'24.6" E in Nov 2015.

Electrochemical procedures. Chronoamperometric and voltammetric experiments were performed with a *Bio-Logic* VSP potentiostat in a three electrode configuration using a Ag|AgCl|$KCl_{sat.}$ reference electrode. All potentials are reported *versus* a reversible hydrogen electrode (E_{RHE} = – 0.197 – 0.059pH *vs.* Ag|AgCl). Auxiliary electrode (high surface area titanium wire) was isolated from the main compartment behind a glass frit (10-16 µm pore size). F:SnO_2 glass with 4 mm × 4 mm electroactive area defined by laser-engraving (*Universal Laser Systems, Inc.*, VersaLaser VLS350) and polyimide (Kapton) tape or glassy carbon disk (3 mm diameter; *BAS*) was used as a working electrode. F:SnO_2 pieces were cleaned by aqua regia and subsequently copiously washed with H_2O (see Ref.[14] for details). Glassy carbon electrode was polished with 0.6 µm Al_2O_3 aqueous paste, sonicated in H_2O, wiped with a clean polishing pad, and sonicated again for *ca* 10 s in RO H_2O. Electroreduction experiments were undertaken after deaeration of the solutions with high purity Ar for 15 min (solution volume *ca* 5 ml).
Quantification of O_2 evolved during water oxidation experiments was undertaken in a flow setup described by Hoogeveen *et al*.[25] A custom-made gas-tight electrochemical cell (PEEK/quartz body) was connected to a mass-flow controller (*Bronkhorst EL Flow Select*) and a molecular oxygen microsensor (*Unisense OX-500*) using *Swagelok* PFA tubing, PTFE and stainless steel connectors. The working and auxiliary electrode compartments were separated by a Teflon fabric reinforced Nafion membrane (N324). Ag|AgCl|KCl(sat.) (*CHI*) and high-surface area nickel foam (*Marketech International*) were used as reference and auxiliary electrodes, respectively. High-purity argon (O_2 < 10 ppm) was fed at a precisely controlled flow of 3 ml min^{-1} through the electrolyte solution and then through the sensor. To achieve reliable response, these experiments were undertaken with higher concentrations of the catalyst precursors, *viz*. 225 µM Fe + 10 µM Pb, in 0.2 M Na_2SO_4 (pH 2.9). Calibration of the setup was undertaken during galvanostatic oxidation of aqueous 1 M KOH using a low surface area nickel wire (99.9%, *Sigma-Aldrich*).

ICP-OES. Analysis was undertaken with a Perkin-Elmer ICP-OES instrument. The samples were diluted to adjust the analyte to within the ideal concentration range, HNO_3 was added and the samples were spiked with Sc and Rh cations as internal standards to monitor instrumental drift. Raw analyte counts were standardised by means of a calibration curve constructed through systematic dilutions of commercially available stock solutions, with all dilutions based on mass. Analysis of solutions prepared using RO purified water as a sample were used to measure the background/baseline and these counts were subtracted from all measurements. The detection limits (in µM) under employed conditions were as follows: Ca <0.5, Mg <0.5, Zn <0.1, Al <0.6, Pb <0.1, Cr <0.1, Fe <0.1, Mn <0.1, Co <0.2, Ni <0.1, Ti <0.1, Mo <0.4, and Sn <0.3.

Scanning Electron Microscopy and Energy Dispersive X-ray analysis. Scanning electron micrographs were recorded on a FEI Magellan 400 FEGSEM equipped with a Bruker Quantax silicon drift detector for EDX analysis. Glass electrode pieces were adhered to stubs using cyanoacrylate and electrical connection was made with a Cu tape. No conductive coating was applied to the samples.

X-ray Photoelectron Spectroscopy. XPS analysis was performed using an AXIS Ultra DLD spectrometer (*Kratos Analytical Inc.*) with a monochromated Al K_α source at a power of 180 W (15 kV × 12 mA), a hemispherical analyser operating in the fixed analyser transmission mode and the standard aperture (analysis area: 0.3 mm × 0.7 mm) The total pressure in the main vacuum chamber during analysis was typically between 10^{-9} and 10^{-8} mbar. Each specimen was analysed at an emission angle of 0° as measured from the surface normal. Assuming typical values for the electron attenuation length of relevant photoelectrons the XPS analysis depth (from which 95 % of the detected signal originates) ranges between 5 and 10 nm for a flat surface.Binding energies were referenced to the C 1s peak at 284.8 eV (adventitious hydrocarbon). The accuracy associated with quantitative XPS is 10-15%.

Acknowledgements

The work was funded by the Australian Research Council *via* the Centre of Excellence for Electromaterials Science (Grant No. CE140100012), Deutsche Forschungsgemeinschaft (SPP 1601 to SAB) and the Deutscher Akademischer Austauschdienst (to KLA). The authors acknowledge Prof. J. Brugger and Dr. B. Etschmann for providing the natural water samples from Australia (Luina and Queenstown, Tasmania), and Prof. Y.-B. Cheng for providing the sample from China (East Lake, Wuhan), all three are from Monash University. The authors also acknowledge the Monash Centre for Electron Microscopy for providing microscopy facilities and Dr. M. Raveggi (Monash University) for assistance with the ICP-OES analysis.

Keywords: water oxidation • natural water • self-healing catalyst • acidic solution

[1] H. Dau, C. Limberg, T. Reier, M. Risch, S. Roggan, P. Strasser, *ChemCatChem* **2010**, *2*, 724-761.
[2] J. H. Montoya, L. C. Seitz, P. Chakthranont, A. Vojvodic, T. F. Jaramillo, J. K. Nørskov, *Nat. Mater.* **2017**, *16*, 70-81.
[3] C. C. L. McCrory, S. Jung, I. M. Ferrer, S. M. Chatman, J. C. Peters, T. F. Jaramillo, *J. Am. Chem. Soc.* **2015**, *137*, 4347-4357.
[4] a) M. W. Kanan, D. G. Nocera, *Science* **2008**, *321*, 1072-1075; b) Y. Surendranath, M. Dinca, D. G. Nocera, *J. Am. Chem. Soc.* **2009**, *131*, 2615-2620; c) D. G. Nocera, *Acc. Chem. Res.* **2012**, *45*, 767-776.
[5] M. Dinca, Y. Surendranath, D. G. Nocera, *Proc. Natl. Acad. Sci. U. S. A.* **2010**, *107*, 10337-10341.
[6] M. Huynh, D. K. Bediako, D. G. Nocera, *J. Am. Chem. Soc.* **2014**, *136*, 6002-6010.
[7] S. Anantharaj, S. R. Ede, K. Sakthikumar, K. Karthick, S. Mishra, S. Kundu, *ACS Catalysis* **2016**, *6*, 8069-8097.
[8] A. M. Ullman, Y. Liu, M. Huynh, D. K. Bediako, H. Wang, B. L. Anderson, D. C. Powers, J. J. Breen, H. D. Abruña, D. G. Nocera, *J. Am. Chem. Soc.* **2014**, *136*, 17681-17688.
[9] L. Trotochaud, S. L. Young, J. K. Ranney, S. W. Boettcher, *J. Am. Chem. Soc.* **2014**, *136*, 6744-6753.
[10] I. Roger, M. D. Symes, *J. Am. Chem. Soc.* **2015**, *137*, 13980-13988.

[11] M. Liu, Y. Yang, X. Yun, M. Zhang, Q. X. Li, J. Wang, *Ecotoxicology* **2014**, *23*, 92-101.
[12] S. A. Bonke, M. Wiechen, R. K. Hocking, X.-Y. Fang, D. W. Lupton, D. R. MacFarlane, L. Spiccia, *ChemSusChem* **2015**, *8*, 1394-1403.
[13] I. Zaharieva, P. Chernev, M. Risch, K. Klingan, M. Kohlhoff, A. Fischer, H. Dau, *Energy Environ. Sci.* **2012**, *5*, 7081-7089.
[14] S. A. Bonke, A. M. Bond, L. Spiccia, A. N. Simonov, *J. Am. Chem. Soc.* **2016**, *138*, 16095-16104.
[15] M. Huynh, C. Shi, S. J. L. Billinge, D. G. Nocera, *J. Am. Chem. Soc.* **2015**, *137*, 14887-14904.
[16] J. Strähle, E. Schweda, *Jander/Blasius: Lehrbuch der analytischen und präparativen Anorganischen Chemie*, 16th ed., S. Hirzel Verlag GmbH & Co., Stuttgart, **2006**.
[17] M. W. Louie, A. T. Bell, *J. Am. Chem. Soc.* **2013**, *135*, 12329-12337.
[18] a) M. D. Merrill, R. C. Dougherty, *J. Phys. Chem. C* **2008**, *112*, 3655-3666; b) K. Yan, Y. Lu, W. Jin, *ACS Sustainable Chem. Eng.* **2016**, *4*, 5398-5403.
[19] A. J. Esswein, Y. Surendranath, S. Y. Reece, D. G. Nocera, *Energy Environ. Sci.* **2011**, *4*, 499-504.
[20] a) M. Huynh, T. Ozel, C. Liu, E. C. Lau, D. G. Nocera, *Chem. Sci.* **2017**, *8*, 4779-4794; b) T. Reier, H. N. Nong, D. Teschner, R. Schlögl, P. Strasser, *Adv. Energy Mater.* **2017**, *7*, 1601275.
[21] R. Frydendal, E. A. Paoli, I. Chorkendorff, J. Rossmeisl, I. E. L. Stephens, *Adv. Energy Mater.* **2015**, *5*, 1500991.
[22] J. S. Mondschein, J. F. Callejas, C. G. Read, J. Y. C. Chen, C. F. Holder, C. K. Badding, R. E. Schaak, *Chem. Mater.* **2017**, *29*, 950-957.
[23] J. Wu, M. Liu, K. Chatterjee, K. P. Hackenberg, J. Shen, X. Zou, Y. Yan, J. Gu, Y. Yang, J. Lou, P. M. Ajayan, *Adv. Mater. Interfaces* **2016**, *3*, 1500669.
[24] L. G. Bloor, P. I. Molina, M. D. Symes, L. Cronin, *J. Am. Chem. Soc.* **2014**, *136*, 3304-3311.
[25] a) D. A. Hoogeveen, M. Fournier, S. A. Bonke, X.-Y. Fang, A. J. Mozer, A. Mishra, P. Bäuerle, A. N. Simonov, L. Spiccia. *Electrochim. Acta* **2016**, *219*, 773–780; b) D. A. Hoogeveen, M. Fournier, S. A. Bonke, A. Nattestad, A. Mishra, P. Bäuerle, L. Spiccia, A. J. Mozer, A. N. Simonov, *J. Phys. Chem. C* **2017**, *121*, 25836–25846.

FULL PAPER

Detailed electrochemical analysis of natural water samples contaminated with transition metal ions shows that this environment is unfavourable for electrocatalytic water splitting, notwithstanding the theoretical possibility to produce efficient catalysts from such contaminants. However, *in situ* generation of a metastable FePb-based water oxidation catalyst at overpotentials 0.8 V and above is demonstrated in slightly acidic natural and pure water.

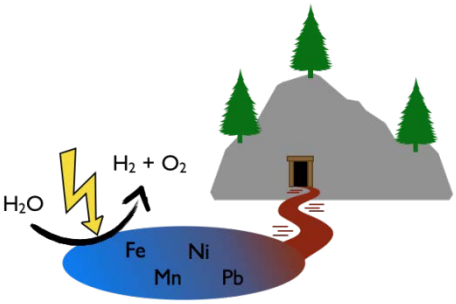

*S. A. Bonke, K. L. Abel, D. A. Hoogeveen, M. Chatti, T. Gengenbach, M Fournier, L. Spiccia, and A. N. Simonov**

Page No. – Page No.

Electrolysis of natural waters contaminated with transition metal ions: identification of a metastable FePb-based oxygen evolution catalyst operating in weakly acidic solutions